

Free-Radical Copolymerization of Styrene and Diethyl Fumarate. Penultimate-Unit Effects on Both Propagation and Termination Processes

Yung-Dae Ma* and Ki-Su Sung

Department of Polymer Science and Engineering, Dankook University, San 8, Hannam-dong, Yongsan-ku, Seoul 140, Korea

Yoshinobu Tsujii and Takeshi Fukuda*

Institute for Chemical Research, Kyoto University, Uji, Kyoto 611-0011, Japan

Received July 31, 2000; Revised Manuscript Received April 27, 2001

ABSTRACT: The propagation and termination processes of the bulk copolymerization of styrene (1) and diethyl fumarate (2) at 40 °C were examined on the basis of a complete set of experimental data obtained by rotating sector and other experiments. The composition curve conformed to the terminal model with a standard deviation of about 1.5%. However, an exceptionally strong penultimate-unit effect (PUE) for the propagation of the terminal radical 1 ($s_1 = k_{211}/k_{111} = 0.055$) was observed. The measured termination rate constants were describable by the penultimate termination model with a geometric mean approximation, showing that a strong PUE exists also on the termination of the terminal radical 1 ($\delta_1 = (k_{121\cdot 21}/k_{111\cdot 11})^{1/2} = 0.067$). The geometric mean approximation was justified by the shielding effect arguments. These analyses suggest that the frequency factors of the propagation and termination rate constants are somehow correlated with each other. On the basis of these results, a general, yet simple two-parameter rate-of-copolymerization equation with PUEs on both propagation and termination was proposed, which described the experiments extremely well. This new rate equation includes the classical Russo–Munari equation as a special case.

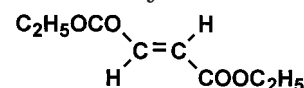
1. Introduction

Since our 1985 rotating-sector (RS) work on a styrene (S)/methyl methacrylate (MMA) system,^{1a} a number of free radical copolymerizations^{1–8} have been studied with respect to the rate constants of propagation \bar{k}_p and termination \bar{k}_t by RS, ESR (electron spin resonance), and PLP (pulsed laser polymerization), establishing that the penultimate-unit effect (PUE) on \bar{k}_p is a general rule rather than an exception.⁹ The origin of this PUE has been an issue of extensive discussion.^{9–11}

More than 3 decades ago, the PUE on the termination step was modeled by Russo and Munari,¹³ who claimed the necessity of considering at least the last two monomer units at the active chain end to interpret rate of copolymerization (R_p) vs composition curves. In most cases, it is only the propagation step that needs to be interpreted by the penultimate model. However, in a recent review,^{9b} we examined the \bar{k}_t vs f curves of various copolymerizations in light of several termination models and suggested the importance of the PUE termination model. More recently, Buback and Kowolik⁸ also noted a good fit of the k_t data of some acrylate/(meth)acrylate copolymerizations by this model.

In this paper, we present full details of a RS study on the bulk copolymerization of S and diethyl fumarate (DEF: Scheme 1) at 40 °C, whose preliminary result was briefly highlighted in the previous review.^{9b} This system is particularly interesting because it exhibits an exceptionally strong PUE on \bar{k}_t as well as on \bar{k}_p . The termination rate constant of DEF¹⁴ is more than 3 orders of magnitude smaller than that of S, which has

Scheme 1. Diethyl Fumarate (DEF)



allowed us to determine the propriety of termination models with little ambiguity. A new two-parameter R_p equation will be proposed, which takes account of PUEs on both \bar{k}_p and \bar{k}_t .

2. Propagation and Termination Models

In this section, we give a brief summary of the models to be discussed in this paper. For more details, see refs 9a,b.

The Penultimate Propagation Model. The penultimate propagation model is characterized by four kinds of propagating radicals ij ($i, j = 1$ or 2), where i and j denote the penultimate and the terminal unit, respectively. This model defines eight propagation rate constants k_{ijm} , where k_{ijm} is the rate constant for the radical ij to add to monomer m ($i, j, m = 1$ or 2); the four monomer reactivity ratios r_{11} , r_{21} , r_{22} , and r_{12} and the two radical reactivity ratios s_1 and s_2 are defined by

$$r_{ii} = k_{iii}/k_{ijj} \quad (i, j = 1 \text{ or } 2; i \neq j) \quad (1)$$

$$r_{ji} = k_{jii}/k_{jjj} \quad (i, j = 1 \text{ or } 2; i \neq j) \quad (2)$$

$$s_i = k_{jii}/k_{iii} \quad (i, j = 1 \text{ or } 2; i \neq j) \quad (3)$$

* To whom correspondence should be addressed.

The copolymer composition $F_1 (= 1 - F_2)$ and the

propagation rate constant \bar{k}_p are given by

$$F_1 = \frac{f_1(\bar{r}_1 f_1 + f_2)}{f_1(\bar{r}_1 f_1 + f_2) + f_2(\bar{r}_2 f_2 + f_1)} \quad (4)$$

$$\bar{k}_p = \frac{\bar{r}_1 f_1^2 + \bar{r}_2 f_2^2 + 2f_1 f_2}{(\bar{r}_1 f_1 / \bar{k}_{11}) + (\bar{r}_2 f_2 / \bar{k}_{22})} \quad (5)$$

where $f_1 (= 1 - f_2)$ is the feed monomer composition and

$$\bar{r}_1 = r_{21}(r_{11}f_1 + f_2)/(r_{21}f_1 + f_2) \quad (6)$$

$$\bar{k}_{11} = k_{111}(r_{11}f_1 + f_2)/(r_{11}f_1 + s_1^{-1}f_2) \quad (7)$$

To obtain \bar{r}_2 and \bar{k}_{22} , exchange 1 and 2 in eqs 6 or 7.

The relative concentration p_i of the terminal radical i is given by

$$p_1 = 1 - p_2 = \frac{(\bar{r}_1 f_1 / \bar{k}_{11})}{(\bar{r}_1 f_1 / \bar{k}_{11}) + (\bar{r}_2 f_2 / \bar{k}_{22})} \quad (8)$$

whereas the relative concentration p_{ij} of the radical ij is given by

$$p_{11} = p_1 - p_{21} = (r_{11}f_1 p_1)/(r_{11}f_1 + s_1^{-1}f_2) \quad (9)$$

To obtain p_{22} and p_{12} , exchange 1 and 2 in eq 9.

The corresponding expressions for the terminal model are obtained by setting $r_{11} = r_{21} = \bar{r}_1 = r_1$, $r_{22} = r_{12} = \bar{r}_2 = r_2$, and $s_1 = s_2 = 1$; hence $\bar{k}_{11} = k_{111} = k_{11}$, etc.

Termination Models. The termination rate constant \bar{k}_t of copolymerization should generally be a function of certain mean properties of the growing chains. The "ideal diffusion" model of Atherton and North¹⁵ gives \bar{k}_t as a linear combination of the k_{ti} 's ($i = 1$ or 2) of the two homopolymerizations:

$$\text{model 1a: } \bar{k}_t = F_1 k_{t1} + F_2 k_{t2} \quad (10)$$

where $F_1 (= 1 - F_2)$ is the copolymer composition. However, if diffusion is rate-controlling, it may be physically more reasonable to assume that \bar{k}_t is inversely proportional to the friction coefficient ξ of the chain.¹⁶ With other conditions being assumed to be the same, averaging ξ with respect to copolymer composition gives¹⁷

$$\text{model 1b: } \bar{k}_t^{-1} = F_1 k_{t1}^{-1} + F_2 k_{t2}^{-1} \quad (11)$$

In models 1 and 2, the diffusional motion of the whole chain or a sufficiently long portion of the chain end whose mean property is representable by F_i is assumed to be important to determine \bar{k}_t .

In the other extreme is the model in which only the terminal unit of the growing chain is assumed to play the main role. This model generally reads

$$\begin{aligned} \text{model 2a: } \bar{k}_t &= \sum_i \sum_j p_i p_j k_{tij} \quad (i, j = 1 \text{ or } 2) \\ &= p_1^2 k_{t1.1} + p_2^2 k_{t2.2} + 2p_1 p_2 k_{t1.2} \end{aligned} \quad (12)$$

where $p_1 (= 1 - p_2)$ is given by eq 8, and k_{tij} is the termination rate constant between radicals i and j ($i, j = 1$ or 2). The Walling cross-termination factor ϕ is defined by $\phi = k_{t1.2}/(k_{t1.1}k_{t2.2})^{1/2}$.¹⁸ However, the intro-

duction of this "adjustable" parameter has often rendered the involved physics obscure.^{9a} If "chemistry" or a certain energetic interaction is important, one would expect the approximate relation $k_{t1.2} = (k_{t1.1}k_{t2.2})^{1/2}$ or $\phi = 1$ to hold. With this geometric mean approximation, eq 12 is simplified to

$$\text{model 2b: } \bar{k}_t^{1/2} = p_1 k_{t1.1}^{1/2} + p_2 k_{t2.2}^{1/2} \quad (13)$$

If, on the other hand, the diffusional motion of the terminal unit is rate-controlling, it should approximately hold that $k_{t1.2} = (k_{t1.1} + k_{t2.2})/2$ (the algebraic mean approximation), and we have

$$\text{model 2c: } \bar{k}_t = p_1 k_{t1.1} + p_2 k_{t2.2} \quad (14)$$

Between these two extremes (models 1 and 2) can there be a vast number of models in which the physical/chemical details of growing copolymer chains are taken into account to different degrees. In light of the current consensus (in homopolymerizations) that termination in the dilute regime is controlled by segmental, rather than translational, diffusivity,¹⁹ the first simplest model to be considered would be the penultimate termination model. The general form of this model reads

$$\text{model 3a: } \bar{k}_t = \sum_i \sum_j \sum_k \sum_l p_{ij} p_{kl} k_{tij. kl} \quad (i, j, k, l = 1 \text{ or } 2) \quad (15)$$

In eq 15, p_{ij} is the relative concentration of type ij radicals (eq 9), and $k_{tij. kl}$ is the k_t between radicals ij and kl . This model defines 16 different rate constants, but application of the geometric mean approximation, viz., $k_{tA.B} = (k_{tA.A}k_{tB.B})^{1/2}$, simplifies eq 15 to^{9b,13}

$$\text{model 3b: } \bar{k}_t^{1/2} = k_{t11.11}^{1/2}(p_{11} + \delta_1 p_{21}) + k_{t22.22}^{1/2}(p_{22} + \delta_2 p_{12}) \quad (16)$$

$$\delta_1 = (k_{t21.21}/k_{t11.11})^{1/2} \quad (17)$$

$$\delta_2 = (k_{t12.12}/k_{t22.22})^{1/2} \quad (18)$$

Application of the algebraic mean approximation, viz., $k_{tA.B} = (k_{tA.A} + k_{tB.B})/2$, simplifies eq 15 to^{9b}

$$\text{model 3c: } \bar{k}_t = k_{t11.11}(p_{11} + \delta_1^2 p_{21}) + k_{t22.22}(p_{22} + \delta_2^2 p_{12}) \quad (19)$$

with δ_i as defined by eqs 17 and 18.

3. Experimental Section

Commercially obtained monomers S and DEF, initiators 2,2'-azobis(isobutyronitrile) (AIBN) and 2,2'-azobis(cyclohexane-1-carbonitrile) (ACN; Nacalai Tesque, Japan), and inhibitor 4-hydroxy-2,2,6,6-tetramethylpiperidiny-1-oxyl (HTMPO; Eastman Kodak Co., Rochester, NY) were purified as described previously.^{1a}

The rate of polymerization initiated by AIBN at 40 °C was determined by the dilatometric method. After polymerization for a given time, the content of the dilatometer was poured into a cold mixture of benzene and petroleum ether (30 wt % benzene for $0.2 < f_1 < 0.8$ and 10 wt % benzene for other values of f_1 , where f_1 is the S mole fraction in the feed monomer mixture). The polymers were further purified by precipitation from a benzene solution into the above-specified solvent

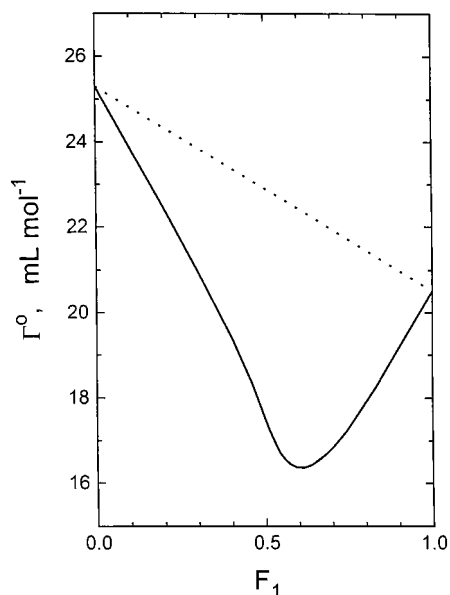


Figure 1. Plot of contraction factor Γ° vs copolymer composition F_1 for the incipient bulk copolymerization of S and DEF at 40 °C (the solid curve, calculated with eq 24 in ref 1a and the volumetric data in Table 1 in this paper). The broken line represents the linear combination.

mixture of benzene and petroleum ether. Copolymer compositions were determined by combustion analysis for carbon.

Other experiments performed involved determining at 40 °C the initiation rate, the volume contraction factor, and the radical lifetime as a function of feed monomer composition. Details of all these experiments were described elsewhere.^{1a} All copolymerization runs were carried out at conversions low enough (<3 wt %) that composition drift with conversion could be neglected.

4. Results

Volume Contraction Factor. The volume contraction factor Γ° for incipient copolymerization was evaluated on the basis of the previously proposed equation.^{1a} Values of the relevant parameters were determined by density measurements. As Figure 1 shows, the values of Γ° thus estimated exhibit large negative deviations from the prediction of the linear combination theory.

Initiation Rate. The effective initiator decomposition rate constant $2f'k_{\text{dec}}$ was determined by the inhibition method using HTMPO. A well-defined inhibition time was obtained for all monomer compositions. The obtained data were fitted to a parabolic function of f_1 by a least-squares method to yield

$$2f'k_{\text{dec}} \times 10^6 = 0.335 - 0.020f_1 + 0.406f_1^2 \quad (\text{in s}^{-1}) \quad (20)$$

Steady-State Polymerization. The rate of copolymerization R_p can formally be expressed by the same equation as for homopolymerization:

$$R_p = (\bar{k}_p/\bar{k}_t^{1/2})R_i^{1/2}[M] \quad (21)$$

$$R_i = 2f'k_{\text{dec}}[I] \quad (22)$$

In this expressions, R_i is the rate of initiation, $[M]$ and $[I]$ are the concentrations of monomers and initiator, respectively, and \bar{k}_p and \bar{k}_t are the propagation and termination rate constants of copolymerization, which generally are a function of composition.^{9a} The proportionality of R_p to $[I]^{1/2}$ was confirmed for $f_1 = 0$ and 0.500.

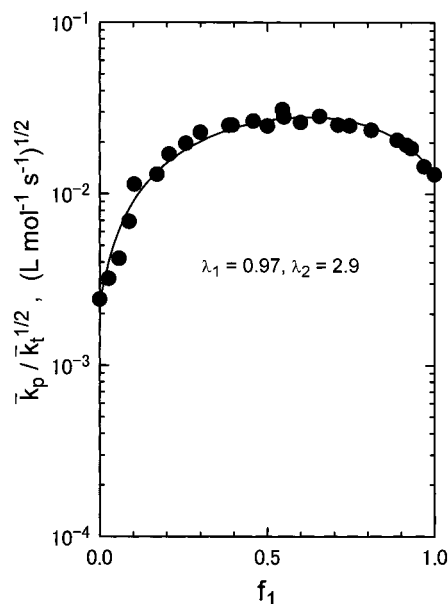


Figure 2. Plot of $\bar{k}_p/\bar{k}_t^{1/2}$ vs f_1 for the S/DEF/AIBN 40 °C system. The solid curve represents eq 27 with $\lambda_1 = 0.97$ and $\lambda_2 = 2.9$.

Figure 2 demonstrates the plot of $\bar{k}_p/\bar{k}_t^{1/2}$ vs f_1 . It can be seen that $\bar{k}_p/\bar{k}_t^{1/2}$ has a maximum value at about $f_1 = 0.5$ and that the $\bar{k}_p/\bar{k}_t^{1/2}$ value of S is about 5 times larger than that of DEF. These results are similar to those reported by Horie et al.²⁰ but differ from those reported by Walling and McElhill²¹ and by Otsu et al.,^{22,23} in which R_p increases monotonically with increasing f_1 , and the R_p of S is more than 8 times larger than that of DEF. This difference, as commented by Horie et al.,²⁰ may be due to the difference of the techniques used for the determination of R_p . (While Horie et al. determined the R_p by differential scanning calorimetry, Walling and McElhill²¹ and Otsu et al.^{22,23} determined the R_p by weighing the polymers isolated from a benzene–petroleum ether mixture and hexane, respectively. Since the molecular weights of DEF homopolymer and DEF-rich copolymers are usually small, oligomeric portions of the samples, particularly those with a high DEF composition, might have been lost without being precipitated, thus causing underestimation of R_p for a relevant range of f_1 .²⁰) The solid curve in Figure 2 is the best-fit representation of the data to the equation proposed later (eq 27, see below), which will be used for the following analysis. Incidentally, if we analyze these data according to the Walling equation,¹⁸ we obtain f_1 -dependent values of the cross-termination factor ϕ ranging from about 4 to about 30. These values have no physical significance, since the Walling equation is based on the terminal propagation model, which is inapplicable to this system (see below).

Radical Lifetime. The radical lifetime τ was determined by the rotating-sector method with ACN as a photosensitizer (for the details of experiments, see ref 1a). Figure 3 shows typical examples of the \bar{R}_p/R_{pL} vs $\log t_L$ plot, where \bar{R}_p is the average rate of polymerization under intermittent illumination of light time t_L and dark time t_D ($t_D/t_L = 2$, in this case), and R_{pL} is the rate under steady illumination. A well-defined τ could be determined for all values of f_1 examined.

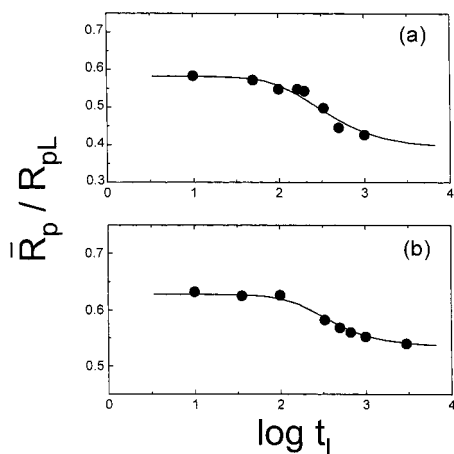


Figure 3. Plot of \bar{R}_p/R_{pL} vs $\log t_L$ for the S/DEF/AIBN/40 °C system: (a) $f_1 = 0$, $[\text{ACN}] = 2.670 \times 10^{-3} \text{ mol L}^{-1}$, and $R_{pD}/R_{pL} = 0.089$ ($\tau = 102.2 \text{ s}$, the solid curve); (b) $f_1 = 0.259$, $[\text{ACN}] = 3.430 \times 10^{-3} \text{ mol L}^{-1}$, and $R_{pD}/R_{pL} = 0.302$ ($\tau = 168.5 \text{ s}$), where R_{pD} is the polymerization rate in the dark.

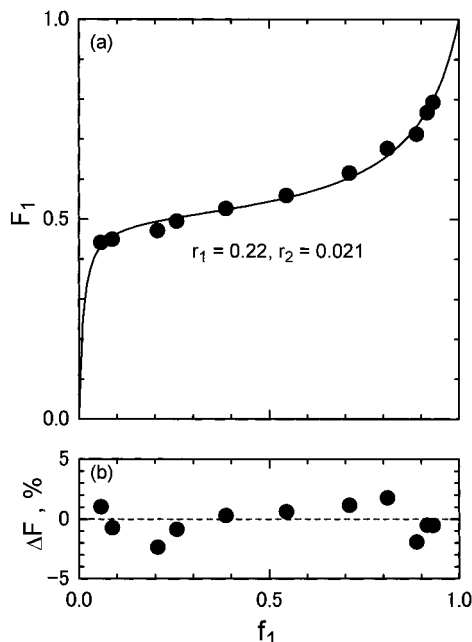


Figure 4. (a) Plot of F_1 vs f_1 for S/DEF copolymers: the filled circles were measured. The solid curve was calculated with the Mayo-Lewis equation²⁴ with $r_{11} = r_{21} = r_1 = 0.220$, and $r_{22} = r_{12} = r_2 = 0.021$; (b) $\Delta F = F_{1,\text{obsd}} - F_{1,\text{calcd}}$ vs f_1 , where $F_{1,\text{obsd}}$ is the observed composition and $F_{1,\text{calcd}}$ is that calculated with Mayo-Lewis equation with the optimum r_1 and r_2 values.

5. Discussion

Composition Curve. The composition data were fitted to the Mayo-Lewis equation (Figure 4).²⁴ An optimum fit was obtained for $r_1 = 0.220$ and $r_2 = 0.021$ with a standard deviation of 1.45%. This deviation is about what would be expectable from the analytical uncertainty (about $\pm 1.5\%$), which means that the composition of this system conforms to the terminal model *within the present experimental error*. In agreement with previous results,^{23,25,26} the $r_1 r_2$ product is very small, showing a highly alternating tendency.

Propagation Process. The values of \bar{k}_p and \bar{k}_t obtained by combining the $k_p/k_p^{1/2}$ and k_p/k_t data are listed in Table 1. As f_1 decreases from 1, \bar{k}_p monotonically decreases in a characteristic fashion, approaching

Table 1. Values of \bar{k}_p and \bar{k}_t for the S(1)/DEF(2)/40 °C System

f_1	$10^2 \bar{k}_p / \bar{k}_t^{1/2} \text{ }^a$ ($\text{L mol}^{-1} \text{ s}^{-1})^{1/2}$	$10^5 \bar{k}_p / \bar{k}_t \text{ }^b$ ($\text{L mol}^{-1} \text{ s}^{-1}$)	\bar{k}_p ($\text{L mol}^{-1} \text{ s}^{-1}$)	$10^{-4} \bar{k}_t$ ($\text{L mol}^{-1} \text{ s}^{-1}$)
0.000	0.241	1.89	0.308	1.63
		1.98	0.294	1.49
0.259	1.87	16.9	2.08	1.23
0.406	2.48	17.5	3.50	2.00
0.515	2.74	12.6	5.96	4.73
0.580	2.81	16.0	4.92	3.08
0.656	2.80	12.0	6.50	5.40
0.749	2.64	9.60	7.27	7.57
0.843	2.31	6.09	8.76	14.4
0.910	1.95	3.59	10.6	29.5
0.951	1.68	1.52	18.5	110
0.983	1.43	0.795	25.8	325
1.000 ^c	1.29	1.40	120	8600

^a Value read from the solid curve in Figure 3. ^b From rotating-sector experiments. ^c From ref 1a.

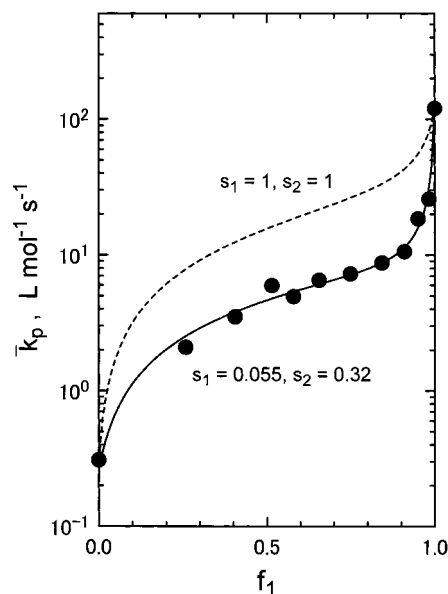


Figure 5. Plot of $\log \bar{k}_p$ vs f_1 for the S/DEF/40 °C system: the circles were measured, and the solid curve shows the penultimate model with $r_{11} = r_{21} = r_1 = 0.220$ and $r_{22} = r_{12} = r_2 = 0.021$, $k_{111} = 120 \text{ L mol}^{-1} \text{ s}^{-1}$, $k_{222} = 0.301 \text{ L mol}^{-1} \text{ s}^{-1}$, $s_1 = 0.055$, and $s_2 = 0.32$; the broken curve shows the terminal model ($s_1 = s_2 = 1$).

the very small value for pure DEF, which is smaller than the S value by a factor about 400.

The broken curve in Figure 5 was calculated with the terminal model (eq 5 with $s_1 = s_2 = 1$, and $\bar{r}_1 = r_1$, etc.), which exhibits large deviations from the experimental values (note the logarithmic ordinate scale). As in many other copolymerization systems, this failure of the terminal model may be ascribed to a PUE. The solid curve in the figure shows the penultimate model with $s_1 = 0.055$ and $s_2 = 0.32$. Thus, the rate constant for a polystyryl radical to add to S is reduced by a factor about 1/20 when the penultimate S unit is replaced by a DEF unit. This is one of the strongest PUEs in propagation that have been reported so far: similarly small values of s_1 were reported by Sato et al., who made ESR studies on the copolymerizations of *p*-tert-butoxystyrene with dibutyl fumarate^{5c} and with dibutyl maleate.^{5d}

Termination Process. Figure 6 shows the plot of $\log \bar{k}_t$ against f_1 . As f_1 decreases from 1, \bar{k}_t decreases drastically at first and then rather gradually. Notably, the DEF \bar{k}_t value is smaller than the S value by a factor

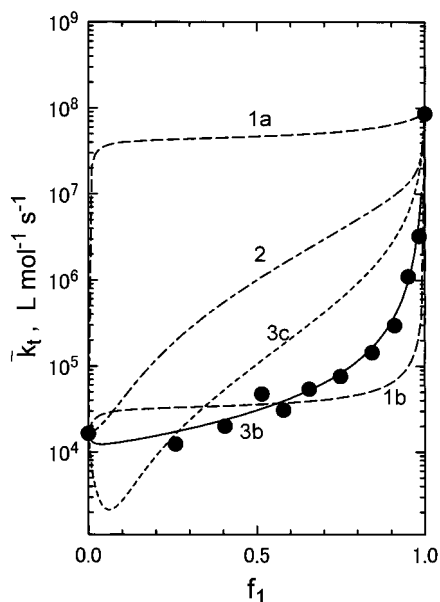


Figure 6. Plot of $\log \bar{k}_t$ vs f_1 for the S/DEF/40 °C system. The circles were measured, and the curves show the models; the broken curves: models 1a (eq 10) and 1b (eq 11); the dot-dash curve: model 2a (eq 12) with $\phi = 0$; the dotted curve: model 3c with $\delta_1 = \delta_2 = 0$ (eq 19); the solid curve: model 3b (eq 16) with $\delta_1 = 0.067$ and $\delta_2 = 0.81$.

of about 5000. Such a large difference in k_t between the two homopolymerizations is inconsistent with the notion of translational diffusion-controlled termination, since translational diffusion constants of polymers do not usually differ so largely (in dilute solution). The exceptionally small value of k_t should be ascribed to the conformational rigidity¹⁴ or the low segmental mobility of PDEF. This interpretation conforms to the current consensus that the termination in the dilute regime is controlled by segmental diffusivity.^{19,27–29} However, the term “diffusivity” used here is still not clear enough physically, and we wish to know more details by comparison of model and experiment. The propriety of a reaction model should be tested with respect to both reproducibility of experimental data and physical acceptability of the parameters deduced by the comparison. One should also be careful enough about the limitation possibly imposed by experimental accuracy. Now we examine the termination models given in section 2 in light of the present \bar{k}_t data.

The two broken curves in Figure 6 show models 1a and 1b, respectively, either of which includes no adjustable parameter. For the reason mentioned above, these models should be understood as representing the diffusional property, not of the center of mass of the whole chain but of a certain portion of the chain including the active chain end. As the figure shows, model 1a is utterly incapable of describing the experiment, while model 1b reproduces the main qualitative feature of the experimental curve. The reason why model 1b is physically more realistic than model 1a was pointed out above. This, in fact, has been justified by the present experiment. However, the significant deviations still existing between the model and experiment indicate that more details of the chain-end properties should be taken into the model.

The terminal termination models (models 2a–2c), in which only the terminal unit is considered, obviously fail to describe the experiment (see the dot-dash curve in Figure 6, which shows model 2a with $k_{1,2} = 0$ or $\phi =$

0, i.e., the smallest physically meaningful limit). This means that at least the last two (or even more) units of the active chain-end should be considered. Model 3a is the general form of the penultimate termination models, and it includes 16 rate constants, while models 3b and 3c are its approximate forms, both of which include the only two parameters δ_1 and δ_2 in common. The failure of model 3c becomes at once clear upon observing that the model with $\delta_1 = \delta_2 = 0$ (the best-fit and smallest physically possible value) gives \bar{k}_t that far deviates from the experimental points (see the dotted curve in Figure 6). On the other hand, model 3b closely fits the experiment in the whole range of f_1 when $\delta_1 = 0.067$ and $\delta_2 = 0.81$ (the solid curve in Figure 6; for a 95% confidence ellipse, see Figure 7). If this analysis is accepted at face value, the penultimate DEF unit has a strong rate-reducing effect on the terminal S radical undergoing radical–radical reactions, while the penultimate S unit has a rather minor effect on the terminal DEF unit.

Mechanistic Consideration on Termination and Propagation Reactions. The above-mentioned success of model 3b seems to provide a new insight into the termination reaction in polymer systems. According to the traditional notion of diffusion-controlled termination, two radicals (or radical sites) in close proximity to each other will necessarily undergo the reaction, its rate constant being determined by the diffusivities of the radicals. Let us assume that type A radicals have a large diffusivity, while those of type B have little diffusivity. The reaction between A's will be fast, while that between B's will be slow. On the other hand, the reaction between A and B will occur still at a high rate, since A can diffuse to B, even when B is fixed in space. In the simplest model in which radicals are modeled by spheres undergoing a Brownian motion, the algebraic mean law holds, i.e., $k_{tA-B} = (k_{tA-A} + k_{tB-B})/2$. This defines one of the idealized limits of radical–radical reactions. In the actual polymer system, the terminal radical will hardly be represented by such a simple model but will be more or less sterically hindered from reacting with other radicals by the atoms, side chains, and main chain of the polymer that it belongs to. Again let us consider the limiting case in which radical B is completely shielded by a steric effect. Then there will be no B–B reaction, or A–B reaction, even if radical A is mobile and unshielded. In this case, the algebraic mean law obviously fails, but the geometric mean law, $k_{tA-B} = (k_{tA-A}k_{tB-B})^{1/2}$, gives the correct answer of $k_{tA-B} = 0$. More generally, we expect that as the shielding effect increases, and the magnitude of k_t becomes smaller, the radical–radical reaction will look more like an activation-controlled reaction rather than a diffusion-controlled one, even though the reaction may not involve a substantial activation energy. In the limit of strong shield, the frequency factor of k_t will, like those of common chemical (activation-controlled) reactions, little depend on the diffusivities of the chains (or chain segments) but will be determined by the strengths of the shielding effects on the two radicals. These effects on the radical–radical reaction may be cooperative to some extent but, as the first-step approximation, they may be assumed to be independent of each other. This is equivalent to writing \bar{k}_t between radicals A and B in the form $\bar{k}_{tA-B} = q_A q_B$, where q_A and q_B denotes the contributions to the frequency factor from the (shielded) radicals A and B, respectively.

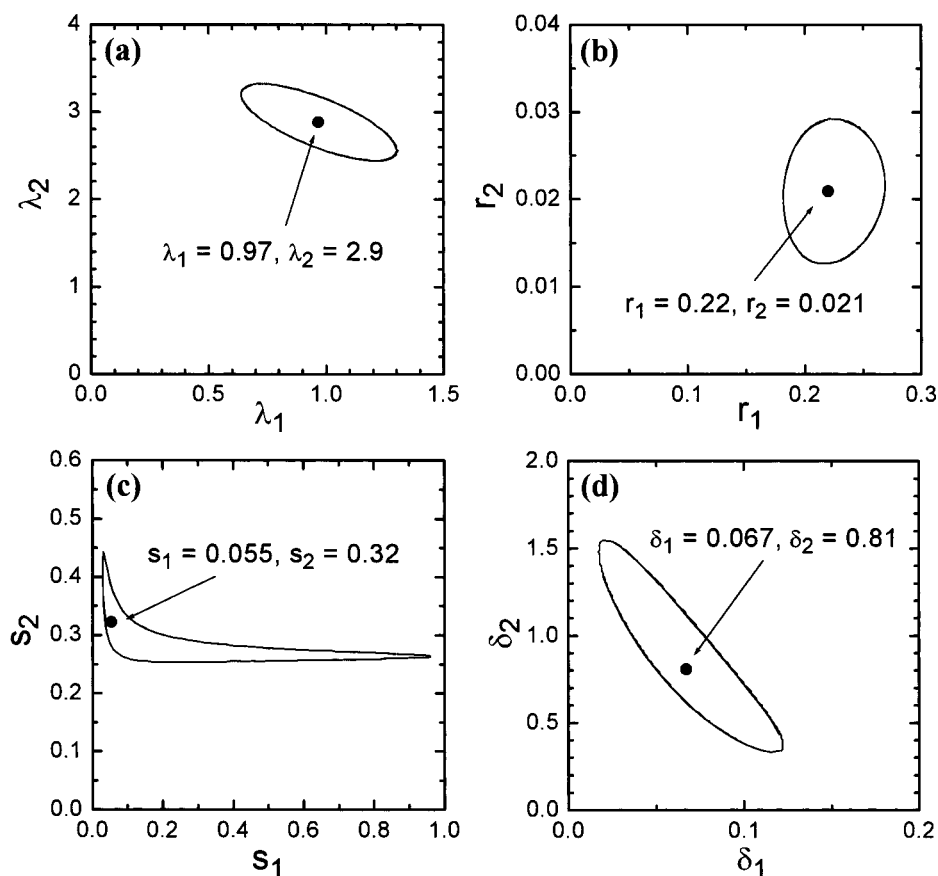


Figure 7. 95% confidence ellipses for (a) λ_i , (b) r_i , (c) s_i and (d) δ_i .

Since the S/DEF system may be understood as being a highly shielded one, the above discussion suggests that $k_{tj\cdot kl}$ may be approximated by the two independent factors q_{ij} and q_{kl} relevant to radicals ij and kl , respectively:

$$k_{tj\cdot kl} = q_{ij}q_{kl} \quad (23)$$

In eq 23, we have neglected the energy factor, as radical–radical reactions are believed to involve essentially no or little energy barrier. It may be easily confirmed that this model gives equivalent results to model 3b, and δ_1 , for example, is given simply by

$$\delta_1 = (k_{t21\cdot 21}/k_{t11\cdot 11})^{1/2} = q_{21}/q_{11} \quad (24)$$

The merit of the model given by eq 23 is that it allows to describe otherwise complicated termination reactions simply in terms of the properties of the individual radicals only. This approximation may also be valid, at least to a limited extent, for the frequency factor of the propagation rate constant, and we tentatively write k_{ijm} in the form^{9b}

$$k_{ijm} = q_{ij}'q_m' \exp(-E_{ijm}/RT) \quad (25)$$

where q_{ij}' and q_m' are the factors relevant to radical ij and monomer m , respectively, and E_{ijm} is the activation energy with R and T being the gas constant and temperature. This model gives, for example,

$$s_1 = k_{211}/k_{111} = (q_{21}'/q_{11}') \exp[-(E_{211} - E_{111})/RT] \quad (26)$$

We previously discussed the origin of PUE on propagation in terms of the “stabilization energy model”, which specifically refers to the energy term in eq 25.^{9a,b,10} The very small value of s_1 observed for the present system is ascribed to either the frequency term or the energy term or both, but no details can a priori be known. However, the above observation that the values of δ_1 ($=0.067$) and s_1 ($=0.055$) are both exceptionally small and similar in order of magnitude suggests that the factors q_{21}'/q_{11}' and q_{21}/q_{11} are somehow correlated with each other and that the main parts of the strong PUEs observed for the propagation and termination processes in the S/DEF system are entropic in origin. The energy term and other factors^{9c} may also play a role in the propagation step, however, so that the close agreement of s_1 and δ_1 should be fortuitous. The importance of the effect of steric shielding on the termination step was also stressed by Buback and co-workers,^{8,19} who, however, observed no correlation between k_t and k_p in acrylate and methacrylate polymerizations. In this regard, the S/DEF system may be rather exceptional for the extremely strong shielding effect. Last but not least, there is even the possibility that this system is governed by the “reaction–diffusion-controlled termination”^{19a} for the extremely low diffusivities of the radicals. By this model, too, the correlation between δ_i and s_i may be interpretable. More experimental and theoretical work is needed before we get a definite general picture of termination and propagation processes.

New Rate-of-Copolymerization Equation. If we combine the general penultimate-propagation eq 5 with the penultimate-termination eq 16 (or eq 15 with eq 23), we obtain, after a somewhat complicated but straight-

forward calculation using eqs 6–9, the following simple expression for the copolymerization rate coefficient $\bar{\omega} = k_p/k_t^{1/2}$:

$$\frac{\bar{r}_1 f_1^2 + \bar{r}_2 f_2^2 + 2f_1 f_2}{\bar{\omega}} = \frac{\bar{r}_1 f_1}{\omega_1} \frac{r_{11} f_1 + \lambda_1 f_2}{r_{11} f_1 + f_2} + \frac{\bar{r}_2 f_2}{\omega_2} \frac{r_{22} f_2 + \lambda_1 f_1}{r_{22} f_2 + f_1} \quad (27)$$

with

$$\omega_i = k_{iif}/k_{tii}^{1/2} \quad (i = 1 \text{ or } 2) \quad (28)$$

$$\lambda_i = \delta_i/s_i \quad (i = 1 \text{ or } 2) \quad (29)$$

Note that eq 27 is remarkably simple including the only two new parameters λ_1 and λ_2 , which are the ratios of the termination and propagation PUE parameters δ_i and s_i . When $\bar{r}_i = r_{ii} = r_i$, eq 27 becomes formally identical with the Russo–Munari equation¹³ in which only the termination PUE was considered in the geometric mean approximation. In other words, eq 27 includes their equation as the special case with $s_i = 1$ or $\lambda_i = \delta_i$ (and $\bar{r}_i = r_{ii} = r_i$) and is expected to have the widest possible applicability of all the rate equations proposed so far.^{9b} Actually, eq 27 describes the rate data of the present system extremely well (see the solid curve in Figure 2: $\lambda_1 = 0.97$ and $\lambda_2 = 2.9$). These best-fit values of λ_i are close, but not exactly equal, to the ratios of the δ_i and s_i values separately estimated ($\delta_1/s_1 = 1.22$ and $\delta_2/s_2 = 2.5$) because of subtle differences in statistical weight to treat different sets of experimental data in the best-fit calculations. In any case, despite the strong PUEs on the individual propagation and termination processes, the PUE on the rate of copolymerization R_p or $\bar{\omega}$ appears only modestly because of the cancellation of the two effects.

As has been described, eq 27 is based on eq 23 (or model 3b), which is valid for strongly shielded systems. When the shielding effects on both radicals A and B are small, the system will be better represented by the diffusion model, and eq 23 (or model 3b) will be no more valid. We expect, however, that both of the homopolymerization k_t 's in such a system will be large and similar in magnitude so that numerical differences between models 3b and 3c will be rather trivial. In effect, eq 27 will work, at least as a good approximation, for every system.

6. Conclusions

Very strong PUEs on both the propagation and termination steps of S/DEF copolymerization were observed. The penultimate termination model with a geometric mean approximation was successfully applied to the experimental data, and this model, combined with the general penultimate propagation model, gave a new two-parameter rate-of-copolymerization equation with a wide possible applicability. The geometric mean approximation was justified by the shielding effect arguments. The frequency factors of the propagation and termination rate constants of the S/DEF system were suggested to be correlated with each other, in this particular system.

It is pleasing to observe that the ESR results reported by Sato et al. for the similar copolymerization systems^{5c,d} are essentially consistent with these conclusions.

Finally, it should be stressed that the fact that penultimate units affect termination is additional evidence for termination being controlled by segmental diffusion in dilute solution.^{19,20,27–29}

Acknowledgment. This work was supported by the Korea Science and Engineering Foundation (KOSEF 941-1100-017-2) and also by a Grant-in-Aid for Scientific Research, the Ministry of Education, Science, Sports, and Culture, Japan (Grant-in-Aid 12450385).

Supporting Information Available: Tables showing results of the density measurements, the inhibition time measurements, the steady-state experiments, and the rotating-sector experiments. This material is available free of charge via the Internet at <http://pubs.acs.org>.

References and Notes

- (1) (a) Fukuda, T.; Ma, Y.-D.; Inagaki, H. *Macromolecules* **1985**, *18*, 17. (b) Ma, Y.-D.; Fukuda, T.; Inagaki, H. *Macromolecules* **1985**, *18*, 26. (c) Fukuda, T.; Kubo, K.; Ma, Y.-D.; Inagaki, H. *Polym. J.* **1987**, *19*, 523. (d) Ma, Y.-D.; Won, Y.-C.; Kubo, K.; Fukuda, T. *Macromolecules* **1993**, *26*, 6766. (e) Ma, Y.-D.; Kim, P.-S.; Kubo, K.; Fukuda, T. *Polymer* **1994**, *35*, 1375.
- (2) (a) Davis, T. P.; O'Driscoll, K. F.; Piton, M. C.; Winnik, M. A. *J. Polym. Sci., Polym. Lett. Ed.* **1989**, *27*, 181. (b) Davis, T. P.; O'Driscoll, K. F.; Piton, M. C.; Winnik, M. A. *Macromolecules* **1990**, *23*, 2113. (c) Davis, T. P.; O'Driscoll, K. F.; Piton, M. C.; Winnik, M. A. *Polym. Int.* **1991**, *24*, 65. (d) Piton, M. C.; Winnik, M. A.; Davis, T. P.; O'Driscoll, K. F. *J. Polym. Sci., Polym. Chem. Ed.* **1990**, *28*, 2097.
- (3) Sanayei, R. A.; O'Driscoll, K. F.; Klumperman, B. *Macromolecules* **1994**, *27*, 5577.
- (4) Olaj, O. F.; Shnöll-Bitai, I.; Kremminger, P. *Eur. Polym. J.* **1989**, *25*, 535.
- (5) (a) Sato, T.; Takahashi, K.; Tanaka, H.; Ohta, T.; Kato, K. *Macromolecules* **1991**, *24*, 2330. (b) Sato, T.; Kawasaki, S.; Seno, M.; Tanaka, H.; Kato, K. *Makromol. Chem.* **1993**, *194*, 2247. (c) Sato, T.; Shimooka, S.; Seno, M.; Tanaka, H. *Macromol. Chem. Phys.* **1994**, *195*, 833. (d) Sato, T.; Katajima, T.; Seno, M.; Hayashi, Y. *J. Polym. Sci., Polym. Chem. Ed.* **1998**, *36*, 1449.
- (6) Schoonbrood, H. A. S.; Van der Reijten, B.; de Kock, J. B. L.; Mander, B. G.; van Herk, A. M.; German, A. L. *Macromol. Rapid Commun.* **1995**, *16*, 119.
- (7) Hutchinson, R. A.; McMinn, J. H.; Paquet, D. A.; Beuermann, S.; Jackson, C. *Ind. Eng. Chem. Res.* **1997**, *36*, 1103.
- (8) Buback, M.; Kowollik, C. *Macromolecules* **1999**, *32*, 1445.
- (9) For reviews, see: (a) Fukuda, T.; Kubo, K.; Ma, Y.-D. *Prog. Polym. Sci.* **1992**, *17*, 875. (b) Fukuda, T.; Ide, N.; Ma, Y.-D. *Macromol. Symp.* **1996**, *111*, 305. (c) Coote, M. L.; Davis, T. P.; Radom, L. *ACS Symp. Ser.* **2000**, *168*, 82. (e) Heuts, J. P. A.; Coote, M. L.; Davis, T. P.; Johnston, L. P. M. *ACS Symp. Ser.* **1998**, *685*, 120.
- (10) Fukuda, T.; Ma, Y.-D.; Inagaki, H. *Makromol. Chem., Rapid Commun.* **1987**, *8*, 495.
- (11) (a) Coote, M. L.; Zammitt, M. D.; Davis, T. P.; Willet, G. D. *Macromolecules* **1997**, *30*, 8182. (b) Coote, M. L.; Johnston, L. P. M.; Davis, T. P. *Macromolecules* **1997**, *30*, 8191. (c) Coote, M. L.; Davis, T. P. *Macromolecules* **1999**, *32*, 3626. (d) Coote, M. L.; Davis, T. P. *Macromolecules* **1999**, *32*, 2935.
- (12) Heuts, J. P. A.; Gilbert, R. G.; Maxwell, I. A. *Macromolecules* **1997**, *30*, 726.
- (13) Russo, S.; Munari, S. *J. Macromol. Sci., Chem.* **1968**, *2*, 1321.
- (14) Otsu, T.; Yamada, B.; Ishikawa, T. *Macromolecules* **1991**, *24*, 415.
- (15) Atherton, J. A.; North, A. M. *Trans. Faraday Soc.* **1962**, *58*, 2049.
- (16) Ito, K.; O'Driscoll, K. F. *J. Polym. Sci., Polym. Chem. Ed.* **1979**, *17*, 3913.
- (17) Ma, Y.-D.; Kim, P.-S.; Kubo, K.; Fukuda, T. *Polymer* **1994**, *35*, 1375.
- (18) Walling, C. *J. Am. Chem. Soc.* **1949**, *71*, 1930.
- (19) (a) Beuermann, S.; Buback, M. *ACS Symp. Ser.* **1998**, *685*, 84. (b) Buback, M. *ACS Symp. Ser.* **2000**, *768*, 39.

- (20) Horie, K.; Mita, I.; Kambe, H. *J. Polym. Sci., Part A-1* **1969**, *7*, 2561.
- (21) Walling, C.; McElhill, E. A. *J. Am. Chem. Soc.* **1951**, *73*, 2819.
- (22) Otsu, T.; Ito, O.; Toyoda, N. *Macromol. Chem., Rapid Commun.* **1981**, *2*, 729.
- (23) Toyoda, N.; Yoshida, M.; Otsu, T. *Polym. J.* **1983**, *15*, 255.
- (24) Mayo, F. R.; Lewis, F. M. *J. Am. Chem. Soc.* **1944**, *66*, 1594.
- (25) Vandenburg, L. F. V.; Brockway, C. E. J. *J. Polym. Sci., Part A-1* **1965**, *3*, 575.
- (26) Lewis, F. M.; Walling, C.; Cummings, W.; Briggs, E. R.; Mayo, F. R. *J. Am. Chem. Soc.* **1948**, *70*, 1519.
- (27) (a) North, A. M.; Read, G. A. *Trans. Faraday Soc.* **1961**, *57*, 859. (b) Benson, S. W.; North, A. M. *J. Am. Chem. Soc.* **1962**, *84*, 935.
- (28) (a) Ito, K. *J. Polym. Sci., Polym. Chem. Ed.* **1972**, *10*, 3159. (b) Mahabadi, H. K.; O'Driscoll, K. F. *J. Polym. Sci., Polym. Chem. Ed.* **1977**, *15*, 283.
- (29) (a) Buback, M. *Macromol. Chem. Phys.* **1990**, *191*, 1575. (b) Buback, M.; Kowollik, C.; Kurz, C.; Wahl, A. *Macromol. Chem. Phys.* **2000**, *201*, 464.

MA001337O